

Niobium direct detectors for fast and sensitive terahertz spectroscopy

M. O. Reese, D. F. Santavicca, D. E. Prober, A. B. True, and C. A. Schmittenmaer

Citation: *Rev. Sci. Instrum.* **78**, 086111 (2007); doi: 10.1063/1.2769575

View online: <http://dx.doi.org/10.1063/1.2769575>

View Table of Contents: <http://rsi.aip.org/resource/1/RSINAK/v78/i8>

Published by the [American Institute of Physics](#).

Related Articles

Optically addressed near and long-wave infrared multiband photodetectors

Appl. Phys. Lett. **100**, 241103 (2012)

Metamaterial metal-based bolometers

Appl. Phys. Lett. **100**, 203508 (2012)

Optical properties of armchair graphene nanoribbons embedded in hexagonal boron nitride lattices

J. Appl. Phys. **111**, 093512 (2012)

Photovoltaic infrared detection with p-type graded barrier heterostructures

J. Appl. Phys. **111**, 084505 (2012)

Mid-wave infrared HgCdTe nBn photodetector

Appl. Phys. Lett. **100**, 161102 (2012)

Additional information on *Rev. Sci. Instrum.*

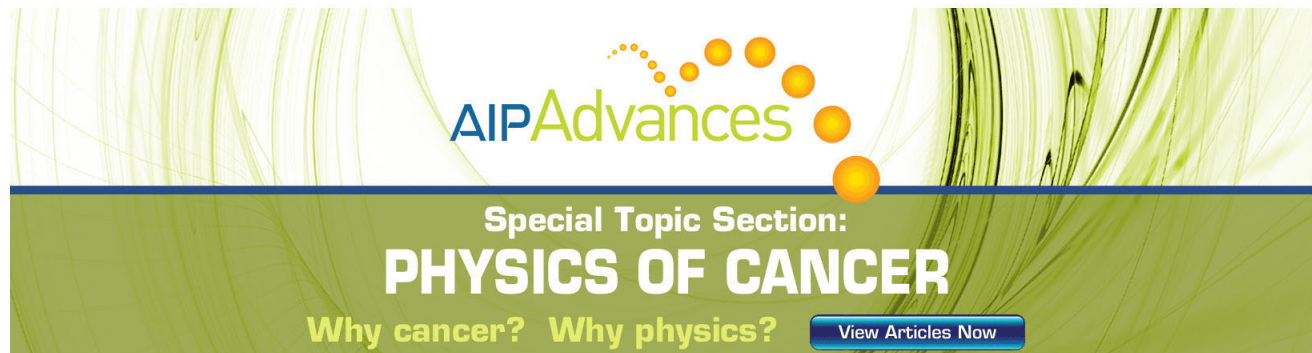
Journal Homepage: <http://rsi.aip.org>

Journal Information: http://rsi.aip.org/about/about_the_journal

Top downloads: http://rsi.aip.org/features/most_downloaded

Information for Authors: <http://rsi.aip.org/authors>

ADVERTISEMENT

The advertisement features a green and yellow abstract background with flowing lines. At the top, the text 'AIPAdvances' is displayed in a green, sans-serif font, with a series of orange dots of varying sizes arranged in a curved path above it. Below this, the text 'Special Topic Section:' is written in a smaller, white, sans-serif font. Underneath that, the words 'PHYSICS OF CANCER' are prominently displayed in a large, bold, white, sans-serif font. At the bottom, the phrase 'Why cancer? Why physics?' is written in a yellow, sans-serif font. To the right of this phrase is a blue button with the text 'View Articles Now' in white.

Niobium direct detectors for fast and sensitive terahertz spectroscopy

M. O. Reese, D. F. Santavicca, and D. E. Prober

Department of Applied Physics, Yale University, New Haven, Connecticut 06520-8284

A. B. True and C. A. Schmuttenmaer

Department of Chemistry, Yale University, New Haven, Connecticut 06520-8107

(Received 6 May 2007; accepted 17 July 2007; published online 20 August 2007)

We report the performance of a niobium hot-electron bolometer designed for laboratory terahertz spectroscopy. The antenna-coupled detector can operate above 4.2 K and has fast (subnanosecond) response. Detailed microwave measurements of performance over a wide range of operating conditions were correlated with quantitative terahertz measurements. The maximum responsivity is 4×10^4 V/W with a noise equivalent power at the detector of 2×10^{-14} W/Hz^{1/2}, approaching the intrinsic thermal fluctuation limit for the device. This detector enables a variety of novel laboratory spectroscopy measurements. © 2007 American Institute of Physics. [DOI: 10.1063/1.2769575]

Recent advances in photon detectors enable measurements near the theoretical limits of sensitivity in the terahertz (THz)/far-infrared (FIR) region for the wavelength range of approximately 0.1–1 mm. The most sensitive direct (power) detectors are bolometers developed for astrophysics observations.^{1,2} These detectors are typically slow, with millisecond (msec) response, operate at temperatures below 0.5 K, and have limited but acceptable dynamic range. In a number of laboratory spectroscopy and sensing applications, detectors with reasonable sensitivity but much faster response and larger dynamic range are needed; a more accessible operating temperature is also desirable. We report the development and detailed characterization of a niobium (Nb) hot-electron detector that addresses these needs.

The detector is an antenna-coupled bolometer that uses the superconducting transition to read out the temperature change due to power absorption. Antenna coupling allows a small sensor element, which is more sensitive than a large-area detector. In our case, the absorber also serves as the thermometer element and, due to the antenna-coupling, photons of one polarization are detected. This approach is now well established in the superconducting hot-electron bolometer (HEB) heterodyne mixer.³ Use of such antenna-coupled HEBs as (nonheterodyne) power detectors has not been as well studied. This is the application we investigate. Other power detectors based on absorption in a superconductor or use of a superconductor thermometer have been reported.^{2,5–7} However, none of these achieves the combination of sensitivity and speed of the detector we report.

A detector using the concept we study is reported also as a commercial product.⁸ The noise, presumably for small detected power, is similar to what we measure. This article provides much more detailed performance data for noise and responsivity as well as dependence on detected power and on the operating temperature. With this information, spectroscopy experiments using this detector can be designed with greater confidence. Moreover, we show that the noise for this power detector is determined almost entirely by intrinsic thermal fluctuations.² This conclusion could not be drawn with certainty from heterodyne measurements on similar-size Nb devices⁹ nor from measurements on larger area Nb film

detectors.¹⁰ Our work builds on the extensive and careful measurements of Nb film detectors.¹⁰

Current laboratory THz spectroscopy employs two main approaches. The Fourier-transform IR (FTIR) spectrometer uses a broad band continuous-wave source. A cold Si bolometer is typically used to measure changes in the relatively constant detected power. This requires modest bandwidth (\leq KHz) with good linearity at microwatt power levels. The other main approach is time-domain THz spectroscopy (TDS).⁴ This uses a pulsed, broad band THz source with a gated detector. Frequency components are determined from the electric field versus time on a subpicosecond (psec) timescale. The source and detector are driven by a sub-psec optical pulse. The detector is either a nonlinear crystal or a photoconductive semiconductor. If the THz waveform to be detected has a long duration (>100 ps), these detectors are not optimal. They collect only a small amount of energy in each sample, and the required path length difference is large.

The detector was developed for measurement of THz emission or changes of THz transmission that occur on a nsec to msec timescale, following an initiating event such as an optical pulse. Spectral resolution is accomplished with a tunable external element. We discuss specific applications at the end of this article. The detector response extends to ~ 10 THz or higher,^{9,10} as set by the antenna. Device response was measured with a broad band, pulsed THz source; with a thermal THz source (hot-cold load); and with a time-varying microwave signal. The microwave tests allow accurate calibration of the dissipated power and also allow performance tests varied over a wider range of operating conditions than is convenient in a THz test system. We report the responsivity \mathcal{R} , in V/W, the noise equivalent power (NEP) in W/Hz^{1/2}, and the saturation power (P_{sat}). The NEP indicates the minimum resolvable input power with unity signal to noise in a 1 Hz output bandwidth.

Device fabrication was optimized for this application.¹¹ The active element of the device is a $2.5 \mu\text{m} \times 1 \mu\text{m} \times 12$ nm Nb microbridge with a normal state resistance of $\approx 100 \Omega$ to match the antenna impedance. These dimensions were chosen to obtain good sensitivity, while ensuring opera-

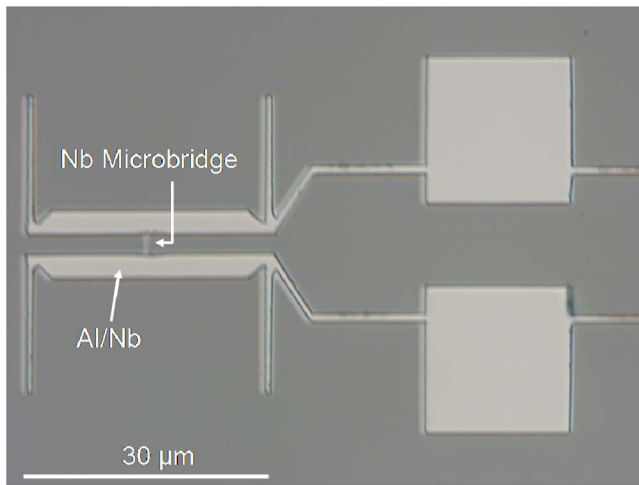


FIG. 1. Optical image of antenna-coupled microbridge and double-dipole antenna; part of the THz choke structure is shown on the right.

tion well below saturation with a room temperature source. The room temperature background couples nanowatt power levels into the detector. A smaller, more sensitive device could be used with a lower background. The Nb microbridge is at the center of a double-dipole antenna designed for coupling between 0.8 and 1.6 THz;¹² see Fig. 1. The antenna consists of 12 nm of Nb covered by 200 nm of Al with a sheet resistance of less than 0.1 Ω/sq . The device is produced on a high-resistivity Si substrate; a hyperhemispherical Si lens focuses the THz signal through the substrate to the antenna. A THz choke structure prevents loss of the THz signal, but allows dc-GHz input and output. Two devices with similar dc properties were studied; one primarily at microwave frequencies and the other at THz frequencies.

Measurements were conducted using two high frequency systems: microwave and THz. In the microwave cryostat an amplitude-modulated microwave signal ($f \approx 1$ GHz; $f_{\text{mod}} = 10\text{--}400$ MHz) is applied and the output at the modulation frequency is amplified by a low noise cryogenic amplifier, followed by a spectrum analyzer.⁹ Negligible room temperature blackbody radiation and IR reach the sample. We first measured the voltage output with $f_{\text{mod}} = 80$ MHz to match the repetition rate of the pulsed THz source (see below). We measured the response and noise at the 50 Ω amplifier input over a wide range of parameters likely to be used in applications. The modulation frequency was varied to determine the output bandwidth of the device. It has a -3 dB bandwidth of 240 MHz, equivalent to a thermal relaxation time of 0.7 ns, and consistent with previous measurements of phonon cooling in similar Nb films.^{9,10} The 80 MHz signal is thus only slightly attenuated by about 5%. Even larger output bandwidths appear possible with improved deposition conditions.¹¹

The microwave measurements show large response and good dynamic range. In the small signal regime, $\mathcal{R}_{\text{max}} = 4 \times 10^4$ V/W at $f_{\text{mod}} = 80$ MHz, obtained for a bath temperature $T_b = 5.2$ K $\approx 0.9T_c$, with $V = 0.2$ mV. The Nb transition temperature is $T_c = 5.8$ K. P_{sat} is defined as the power for which \mathcal{R} is reduced to 50% of its small signal value. For $T_b = 5.2$ K, P_{sat} is 7 nW. These measurements are reproducible to better than 10%. The systematic errors of the microwave measurement are estimated to be $<20\%$, while for the

TABLE I. Device performance vs temperature; responsivity \mathcal{R} and electrical NEP are measured at $P \ll P_{\text{sat}}$. For $T \leq 4.2$ K, the NEP could be reduced $\sim 30\%$ with a lower noise amplifier.

T (K)	\mathcal{R} (kV/W)	P_{sat} (nW)	NEP (10^{-14} W/Hz ^{1/2})
5.2	40	7	2
4.2	10	66	7
3.2	6	120	11

THz measurements, the systematic errors could be a factor of 2. The maximum responsivity at a given T_b approximately follows the empirical relation:

$$\mathcal{R}(P) = \mathcal{R}(P=0) / [1 + (P/P_{\text{sat}})^{3/2}]. \quad (1)$$

P_{sat} increases as the bath temperature T_b is reduced, but the responsivity decreases. For a given absorbed power, \mathcal{R} can be optimized by adjusting the T_b . Using Eq. (1), we estimate that room temperature radiation coupled to the detector can reduce \mathcal{R} 3%–6%. Our findings are summarized in Table I and Fig. 2. The NEP data are discussed below.

The THz-frequency tests were conducted in an optical-access cryostat with a room temperature amplifier. We use antenna coupling.¹² The THz response was tested using a hot-cold load, switching between thermal sources at 315 Hz, as well as using a broad band, pulsed THz source.^{3,13} The hot-cold measurements allow us to apply a known blackbody power external to the cryostat.¹⁴ Assuming a known antenna bandwidth, the power that can be coupled from the hot load to a cold detector is found by integrating the Planck thermal spectrum.¹⁵ For the microwave measurement, we know the coupling and thus \mathcal{R} for power *absorbed* in the device. From this, the optical coupling efficiency η , from the cryostat window to device absorption, is computed to be 0.18.

A broad band, pulsed THz source was used in the other THz tests. It is based on a photoconductive switch driven by a Ti:sapphire laser oscillator.^{4,13} The THz beam is focused onto the Si lens in the cryostat with an off-axis parabolic mirror external to the cryostat. The average THz signal power external to the cryostat in the antenna bandwidth is

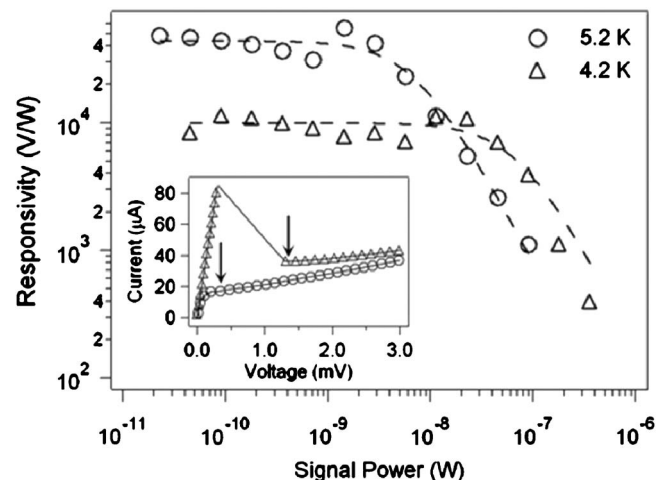


FIG. 2. Responsivity \mathcal{R} vs power with 80 MHz modulation, $T_b = 5.2$ and 4.2 K. Fitted curves are Eq. (1) with parameters of Table I. Inset: I - V curve for $T_b = 5.2$ and 4.2 K, $P = 1$ nW; an arrow points to the location where \mathcal{R} is maximum. There is a 20 Ω dc load line.

TABLE II. Performance of THz direct detectors-Nb antenna-coupled HEB (this work, 5.2 K) and Winston cone for coupled commercial units ($T=4.2$ K) (Ref. 5). The InSb detector is limited to frequencies <1.5 THz for broadband coverage and requires an inhomogenous magnetic field.

	Nb HEB	Si bolometer	Nb film	InSb bolometer
Output bw	240 MHz	1 kHz	200 MHz	≤ 1 MHz
$\text{NEP}^{\text{elec}}(\text{W/Hz}^{1/2})$	2×10^{-14}	2×10^{-13}
$\text{NEP}^{\text{opt}}(\text{W/Hz}^{1/2})$	1.1×10^{-13}	2×10^{-12}	2×10^{-11}	1×10^{-12}

~ 1 nW, based on the hot-cold calibration, and is similar to previous work.¹³ We determined the detector noise and NEP in both measurement systems. The NEP includes contributions from photon shot noise (from room temperature black-body photon background and the signal), from amplifier noise, and from intrinsic device noise.² These contributions add in quadrature. Maximum NEP contribution of the photon shot noise at the detector in the THz setup occurs for $\eta=1$ and is $\sim 0.3 \times 10^{-14} \text{ W/Hz}^{1/2}$; for the microwave setup it is negligible. The photon contribution to the total NEP is thus small. The measured contribution from the amplifier, NEP_{AMP} , is small at $1.0 \times 10^{-14} \text{ W/Hz}^{1/2}$.

The dominant contribution to the calculated NEP is from intrinsic device noise, which is dominated by thermal fluctuations.² $\text{NEP}_{\text{TF}} = (4k_B T^2 G)^{1/2}$, where G is the thermal conductance between the electrons and the substrate/film phonons, and the electron temperature is near T_b . We measured that $G = 1.9 \times 10^{-7} \text{ W/K}$ using Johnson noise thermometry,⁹ giving a predicted $\text{NEP}_{\text{TF}} = 1.9 \times 10^{-14} \text{ W/Hz}^{1/2}$. A smaller microbridge area lowers G and NEP_{TF} , but also lowers P_{sat} .

The electrical NEP is the total NEP for power absorbed in the detector. At 5.2 K in the microwave system, using the known coupling, we measure $\text{NEP}^{\text{elec}} = 2.0 \times 10^{-14} \text{ W/Hz}^{1/2}$. This is consistent with expectation; for the dominant contributions² we predict that $\text{NEP}^{\text{elec}} = [(\text{NEP}_{\text{TF}})^2 + (\text{NEP}_{\text{AMP}})^2]^{1/2} \approx 2.2 \times 10^{-14} \text{ W/Hz}^{1/2}$. The amplifier noise in the THz system is the same. Thus, the optical NEP measured in the THz system, relative to power at the window, is $\text{NEP}^{\text{opt}} = 2.0 \times 10^{-14} / \eta = 1.1 \times 10^{-13} \text{ W/Hz}^{1/2}$. We summarize our findings in Table II and compare to three commercial THz detectors which use different concepts.⁵ The antenna-coupled Nb detector is the most sensitive detector in Table II and is much faster than the semiconductor detectors.

A variety of THz spectroscopic studies on a nsec to msec timescale can be undertaken with the antenna-coupled Nb detector. An example is the measurement of the transient photoconductivity of an ensemble of nanocrystals,⁴ nanowires, or conducting molecules, where it is difficult to attach electrodes. It should also be possible to investigate the dynamic Jahn-Teller effect, which is very sensitive to temperature.¹⁶ Another possible application is the study of protein folding or unfolding using a transmission measurement. The THz probe field couples more strongly to low frequency motion involving secondary and tertiary structures, as compared to a measurement with higher energy photons which couple to localized IR vibrational modes or optical transitions. It is known that the (un)folding dynamics occur on a range of timescales from psecs to msecs or

longer.¹⁷ Indeed, THz studies of proteins¹⁸ and nanocrystals⁴ have been conducted with TDTS methods, but could only investigate dynamics on the psec timescale.

The Nb detector can also be implemented in measurement strategies that have been successfully employed at other photon frequencies. For example, if the detector is coupled with a high-finesse THz cavity, it can function as a far-infrared version of the optical/infrared cavity-ring-down spectrometer⁴ or as the THz version of the Balle-Flygare spectrometer^{4,19} that is now used in the microwave region. Such THz studies would provide information on the structure and dynamics of polar molecules such as water, formaldehyde, hydrogen cyanide, and their hydrogen bonded clusters. This information provides some of the science base for future planetary and astronomical explorations.²⁰ We anticipate that other applications will be undertaken once the initial applications are demonstrated.

We thank L. Frunzio, A. Skalare, P. Peutz, V. Savu, I. Siddiqi, A. Szymkowiak, G. A. Blake, and R. Grober for assistance and discussions. NSF-AST, NSF-DMR, NSF-CHE, NASA GSRP and Yale University supported this work.

¹D. J. Benford and S. H. Moseley, Nucl. Instrum. Methods Phys. Res. A **520**, 379 (2004).

²P. L. Richards, J. Appl. Phys. **76**, 1 (1994).

³M. Hajenius *et al.*, J. Appl. Phys. **100**, 074507 (2006).

⁴C. Schmuttenmaer, Chem. Rev. (Washington, D.C.) **104**, 1759 (2004).

⁵QMC Instruments, Cardiff, UK, www.terahertz.co.uk/QMCI/qmc.html; Si bolometers are also available from Infrared Laboratories, Tucson, AZ.

⁶J. T. Skidmore *et al.*, Appl. Phys. Lett. **82**, 469 (2003); M. Nahum *et al.*, IEEE Trans. Magn. **27**, 3081 (1991); A. J. Kreisler and A. Gaugue, Semicond. Sci. Technol. **13**, 1235 (2000).

⁷A. Luukanen *et al.*, IEEE Microw. Wirel. Compon. Lett. **16**, 464 (2006). The device rf input bandwidth is limited by the inductance of the long strip and is ≈ 0.5 THz.

⁸Insight Product Development, Newton, MA. <http://www.insight-product.com/detect3.html>.

⁹P. J. Burke *et al.*, J. Appl. Phys. **85**, 1644 (1999) and references therein. Here the bandwidth was measured between 0.1–1 GHz.

¹⁰E. N. Grossman, J. E. Sauvageau, and D. G. McDonald, Appl. Phys. Lett. **59**, 3225 (1991).

¹¹M. O. Reese *et al.*, IEEE Trans. Appl. Supercond. **17**, 403 (2007). D. F. Santavicca *et al.*, IEEE Trans. Appl. Supercond. **17**, 412 (2007).

¹²A. Skalare, Th. De Graauw, and H. van de Stadt, Microwave Opt. Technol. Lett. **4**, 9 (1991); A. Skalare (private communication); our antenna does not employ a back reflector. Its coupling bandwidth is roughly estimated to be 0.8–1.6 THz in a Si environment from the published work. If the bandwidth is less than one octave, the value of η would increase, but the electrical NEP would be unchanged.

¹³M. van Exter and D. R. Grischkowsky, IEEE Trans. Microwave Theory Tech. **38**, 1684 (1990).

¹⁴The power delivered at the cryostat window is chopped between a 77 K load, an 8-mm-thick Eccosorb piece of foam dipped in LN₂, and a room temperature absorbing coating on the mechanical chopper wheel, Stycast 2850FT epoxy loaded with 1 mm SiC grains; see M. C. Diez, T. O. Klaassen, C. Smorenburg, V. Kirschner, and K. J. Wildeman, Proc. SPIE **4013**, 129 (2000).

¹⁵A. R. Kerr, IEEE Trans. Microwave Theory Tech. **47**, 325 (1999).

¹⁶C. Testelin *et al.*, Phys. Rev. B **46**, 2183 (1992).

¹⁷H. S. Chung *et al.*, Proc. Natl. Acad. Sci. U.S.A. **102**, 612 (2005) and references therein.

¹⁸A. Markelz *et al.*, Phys. Med. Biol. **47**, 3797 (2002).

¹⁹E. J. Campbell *et al.*, J. Chem. Phys. **74**, 829 (1981).

²⁰G. A. Blake (private communication), see <http://aura.gsfc.nasa.gov/instruments/index.html>